Journal of Engineering Science and Technology
Vol. 16, No. 1 (2021) 052 - 064

X-RAY TRANSMISSION-RATE-MEASURING BY USING LOW-COST LABORATORY COUNTER

AYDIN TARIK ZENGIN

Faculty of Engineering, Computer Science Department,
Istanbul Sabahattin Zaim University, Halkali Cad. No.2, 34303
Halkali, Kucukcekmece, Istanbul, Turkey
E-mail tarik.zengin@izu.edu.tr

Abstract

X-ray transmission rate measurement for material thickness determination is a widely used method in industrial applications. It is usually measured using expensive laboratory equipment. This method, which gives information about the material, is also used quite a lot in medical applications. However, laboratory equipment used in this measurement is often costly. Low-cost laboratory equipment for data acquisition with open-source hardware and software is a lifesaver for the low-budget research projects. Although there are many data acquisition hardware and software in the market, most of them are complex and expensive. They contain many extra features other than some specific ones required for transmission rate measurement. In this study, X-ray transmission rate measurement of some chemical compounds was carried out using a low-cost laboratory counter and data acquisition software. The results are shown by experiments and are consistent with the catalogue values of the materials and chemical compounds used. Thus, in this paper a method is proposed for both measuring the thickness of the material with known linear attenuation coefficient and measuring the linear attenuation coefficient for a material with known thickness.

Keywords: Computerized instrumentation, Data acquisition, Frequency measurement, Pulse measurement, Scintillation counters.

1. Introduction

Low-cost laboratory equipment for experiments is significant for researchers in academia. Since the research budgets are getting tight day by day, it is a logical approach to look into the open-source projects both in software and hardware. One of the equipment that is vital in experiments is a pulse/frequency counter. Some hand-held and bench multimeters, and signal generators provide a counter function. However, they are not convenient to store data and the count-interval, data format, visualization and hardware-control are not adjustable.

Although the necessity of such equipment is clear, not enough study on this issue had been presented. Commercial equipment for this purpose is quite expensive and bulky even though the operation is so simple. Recently, some studies in the laboratory equipment design area had been published. Kim et al. [1] proposed an FPGA-based pulse processing board. Kumar and Malathi [2] designed a synchronous counter using conditional capture FF. Shan et al. [3] proposed a digital frequency discriminator (DFD) using counters. Jurgo et al. [4] proposed a frequency divider using a 6-bit counter. Du et al. [5] proposed a method for frequency measurement based on quantized phase step law. Abdullah et al. [6] used a commercial frequency counter in their psychological stress screening. Amirpour et al. [7] presented a frequency divider based on a counter. Rubiola et al. [8] presented a frequency counter based on linear regression. Another FPGA-based multi-channel frequency counter is proposed by Syahbana et al. [9]. Ritt at el. [10] introduced a GHz waveform digitizer. Beltran [11] presented an ADC data acquisition system with filters. Zahedi [12] proposed a biosignal recorder as an open-source project. Jin and Song [13] developed a sensor monitoring hardware. Real et al. [14] introduced an industrial data acquisition board. Some key specifications for the references given above are shown in Table 1. As the recent improvements and proposed papers show, affordable laboratory equipment is a hot topic. However, there are not much open-source and affordable-in-price alternatives. On the other hand, user-friendly design is a concern since the equipment will be used in a laboratory environment and must be used without much effort.

X-rays that are high-energy photons, lose energy as they pass through a material. If the photons passing through the material can be counted, information about the properties of the material can be obtained. A pulse counter is required for counting these passing through photons. The amount of photons passing through the material is called the transmission rate. The challenge of this work was to measure transmission rate by using affordable counter equipment with adjustable threshold levels, count intervals, data logging functionality, relay interface and network connectivity. In order to meet these needs, an open-source hardware and software pulse/frequency counter prototype is presented by the Zengin [15].

The X-ray mass attenuation coefficients have been determined for energy levels up to MeV long ago [16-18]. Witchjack [19] suggested using tomography for rock-property measurement and fluid-flow visualization using these coefficients. Mass attenuation coefficients of different materials at different energy levels have been measured in many studies [20-28]. Coefficients in bismuth borate glasses were measured by Singh et al. [29]. There are also many studies on the use of X-ray transmission rate measurement in the medical field. Measuring the mass attenuation coefficients of tissues and polymers is of great importance in diagnostics. Various studies have measured the coefficients of human tissues and materials simulating these tissues [30-34]. The use of X-ray transmission rate in the industry is also important. In particular, it is necessary to know the attenuation coefficients of the materials used in the shielding of radioactive sources. X-ray transmission rates of superalloy, concrete and other materials used in shielding have also been measured in various studies [35-41].

Table 1. Key specifications of references.

References	Frequency	Specs.
[1]	20 MHz	FPGA, 10 bits, peak sensing, pulse area sensing, time tag, pulse counter
[2]	2 GHz	Flip-Flop, Clock gating, frequency counter
[3]	NA	Flip-Flop, PLL, ADPLL, frequency discriminator
[4]	10 GHz	Flip-Flop, Frequency divider, jitter removal
[7]	667 MHz	Flip-Flop, Frequency divider, phase shifter
[8]	250 MS/s	FPGA, Linear-regression based, not fully implemented
[9]	10 MHz	FPGA, Built-in calibration, 3 Ch.
[10]	950 MHz	FPGA+DRS, 4 Ch., Complex design, very good SW, Open Source
[11]	15 kS/s	AVR, 8 Ch. multiplexed, UART, SPI, TWI
[12]	500 Hz	AVR, Low frequency, Matlab GUI
[13]	NA	FPGA+ARM, General monitoring purpose, Open Source
[14]	100 Hz	AVR, Very simple design, Open Source

In this paper, X-ray transmission rate measurement of some chemical compounds was performed using the low-cost-laboratory-counter, which is an open-source-hardware and -software frequency/pulse counter circuit and its data acquisition software. It provides a relay interface for external hardware-control. The advantages of the counter design and measurement method presented are that it can be easily implemented, has low error rate, can communicate with other systems via TCP or relay I/O, can save data, and is suitable for use in the research laboratory or industry. In the test environment it was proved to be working up to 10 MHz-frequency pulses, which was quite enough for transmission rate measurement.

2. System Design and Theory

For the convenience of users, the system was designed as a Raspberry Pi (RPi) hat, which makes it easy to use, affordable and portable. Block diagram of the experimental system is shown in Fig. 1. Some early design methods and early-version details are given in the technical report written by the Zengin [15]. An improved version of the hardware and software design with additional features and improvements are being presented in this paper. The most significant improvement, other than minor corrections, is to eliminate the time shift in periodic data acquisition and to add data transmission over TCP. These will be explained in Section 2.2.

An X-ray source of 60 keV was used in the measurements. A (Silicone PhotoMultiplier) SiPM / (Lutetium-yttrium oxyorthosilicate) LYSO detector is located 150cm away from the source. The photons captured in the detector were counted with a pulse counter. The counter was also able to control the experimental setup by keeping the X-ray source open for specified times. The materials to be measured were prepared in blocks of certain thickness. In the experiment, different numbers of blocks were placed between the X-ray source and the sensor and the transmission rate was measured for each.

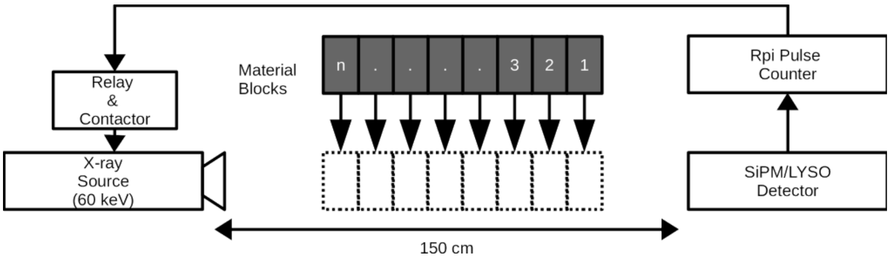

Fig. 1. Experimental system diagram.

2.1. Hardware design

RPi was selected as the base platform as it was a cheap and easy-to-achieve option in the market. Presented system was designed as an RPi expansion hat so that it can be detached any time and give a room for other projects to be implemented on RPi. Other solutions like using MCU timer-interrupts for counting external signals was not considered since the interrupt subroutines block the main process so frequently when the pulse frequency is high, which causes missing pulses. In the presented approach, independent hardware counters were used instead. Hence, neither the counting operation nor the software processes were interrupted. On the other hand, parallel operations with microcontrollers are more difficult as it requires using RTOS. An SBC was preferred instead because it can process both faster and parallel and it is easy to use.

Block diagram of the hardware system is shown in Fig. 2. Input signals were applied to an operational amplifier (opamp) comparator stage and square wave count-signals were created. Hardware counter stage counted and stored the count value until they were collected by RPi. OPA656 wideband opamps were used as the comparators as it provides a low input-noise-voltage and works with high frequency signals up to 500MHz. SN74LV8154 hardware counters received the square wave signals generated by the comparators as clock signals. Reference voltage was set by using the potentiometer connected to inverting input of the opamp. Op-amps were used in single-supply mode since the input signals were always positive and negative output was not desired.

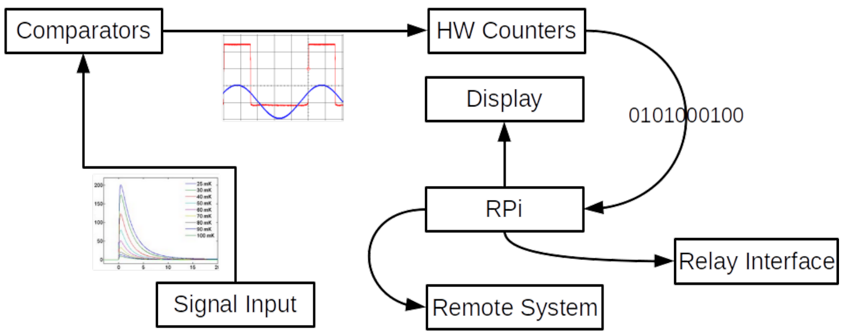

Fig. 2. Block diagram of HW system.

Schematics were shared publicly through GitHub[1] as an open-source project for the benefit of researchers. It can be used, modified, and redistributed freely. It was designed as an RPi hat using the I/O ports and supply voltages directly through the RPi connector for simplicity. Multiple ground (GND) pins were distributed around the board in order to reduce noise generated by vias.

The final product enclosed in a box and powered by a DC battery power source is shown in Fig. 3. Input ports using BNC connectors and relay interface with 9-pin DSUB connector is shown in the figure. Although the system could run on DC power adapter and provide a screen output through the HDMI port, it could also be controlled through remote desktop over Wi-Fi without any cable connected to it. Therefore, presented design could be defined as a portable and lightweight pulse counter system.

Fig. 3 Photo of the enclosed system.

2.2. Software design

Data acquisition software of the system was written in Python language using the Qt graphical library. User interface (UI) shown in Fig. 4 was designed for both mouse and touchscreen operation with big buttons. UI provides dedicated frames, where the count data could be seen in detail, count interval could be set, and button groups for counter start/stop, log saving, and relay interface control with auto-off feature were placed.

All the data acquired from the hardware counters could be saved to a local file to be processed later. Automatic shut-off feature can be used to control the external hardware in the test setups. Thus, it could be ensured that every measurement is taken in the same time interval. The software code was shared publicly on GitHub[2] as an open-source project as it was shared in hardware design. It can freely be shared, modified and redistributed under the GPL license.

Some errors and deficiencies in the software offered in the previous version have been fixed in this version. The first was the time shift that occurred at the time of measurement. The error that caused approximately 1ms of time shift in every 1000ms was corrected by updating the software. The periodic data acquisition code

[1] https://github.com/atzengin/RPi-Frequency-Counter
[2] https://github.com/atzengin/RPi-Frequency-Counter-Software

was completely transformed into a multi-threaded structure triggered by the timer. Another improvement is that the received data can be sent over the network via the TCP protocol. In this way, live data received during the experiment can be transmitted wirelessly to the remote system and processed in real time in Matlab or other tool supporting TCP protocol. These and other minor enhancements are all accessible through GitHub.

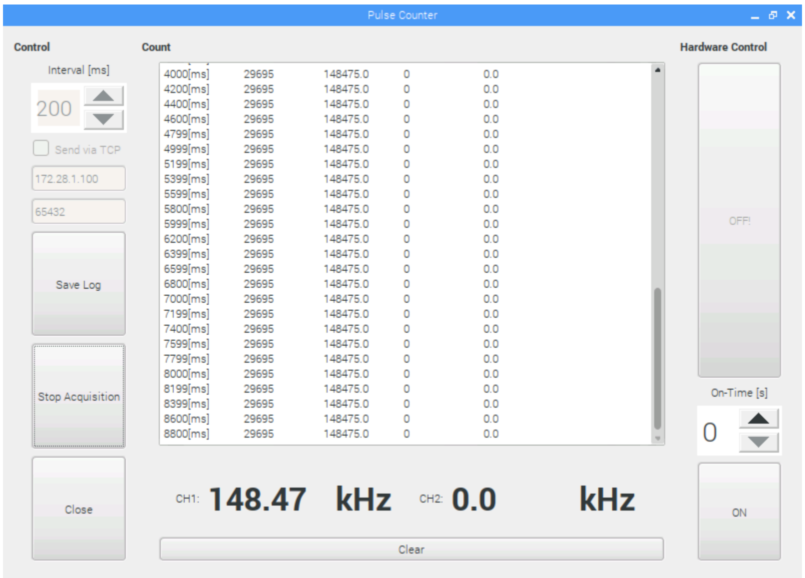

Fig. 4. User interface of frequency/pulse counter.

2.3. Theory of transmission rate

High-energy photons called X-rays lose energy as they pass through a material. Some photons lose their energy and are absorbed. Some of them emerge from the other side at a rate depending on the thickness of the material. The number of photons passing to the other side does not only depend on the energy of the photons and the attenuation coefficient of the material. It is also inversely proportional to the distance of the X-ray source. The further the source is the fewer photons pass through the material. Also, photons scattered from objects in the environment or through the material can reach the sensor simultaneously. In this case, the pile-up situation occurs. Pile-ups are overlapping signals and must be detected during signal processing. These signals may either be ignored or may be tried to be parsed. The former approach is relatively easier, while the latter requires more processing power. In the system presented in this article, pile-up signals are considered as a single photon. The losses that may occur in the photon count for this reason are negligible.

Photon intensity is given in Eq. (1) where μ is the linear attenuation coefficient and x is the photon travel distance in material. As the thickness of the material increases, the intensity of the photons passing to the other side decreases. If the passing photons can be counted, the thickness of the material can be measured. This was where the counter took action in the experiment.

$$I = I_0 e^{-\mu x} \quad (1)$$

Transmission rate measurement is frequently used in industry and medical field. Complex and expensive industry-grade devices are used for measurement. Using these devices in scientific studies increases both cost and complexity. In this study, the transmission rate was measured in a very simple way. An SiPM/LYSO detector detects photons from the X-ray source and produces a nanosecond pulse for each. These pulses are amplified with an operational amplifier before being applied the counter. All the pulses above threshold level are counted by the counter. This count is related to the Intensity (I) given in Eq. (1).

3. Results

The operation of the system is shown in two parts. First, the consistency of the designed counter was demonstrated by an experiment. Then, the transmission ratio of several different materials was measured in an experimental setup.

3.1. Consistency test of the counter

A long time measurement test was performed to demonstrate the consistency of the system. Two signals at 1 MHz and 10 kHz frequencies were applied to the counter channels simultaneously for 5 minutes. During this time, the count was recorded continuously. Signals were created by using a 2 Ch signal generator (AA-Tech AGW-1010). Figures 5 and 6 show the counts with respect to time for Ch1 and Ch2, respectively.

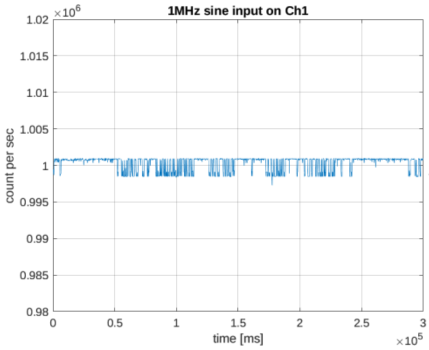

Fig. 5. 1 MHz Signal at Ch1.

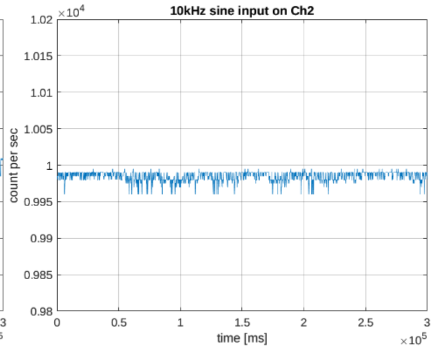

Fig. 6. 10 kHz Signal at Ch2.

Measurements were taken for a long period of time. During this time, the counter counted pulses for each channel for every 200 ms. This interval can be increased or decreased through the GUI. The counts per second are shown in the graphs. As it can be seen from the graphs, deviation was below 0.005% for both channels. This test showed that the system did not deviate for long-term measurements. As the presented design's main objective was being an affordable and customizable pulse counter, the error rate was within acceptable range.

3.2. Transmission rate measurement

X-rays are used to measure the material thickness. There is a relationship between the amount of X-rays passing through the material and the thickness of the material. It is a well-known method used in industry [42]. It is used in many fields of industry such as pipeline maintenance, nuclear applications, concrete inspection, and underground inspection. This method is used when it is desired to measure the thickness of a material without damaging it. Otherwise, it is necessary to measure the thickness of the material by cutting it.

The experimental setup was consisted of an X-ray source, and a gamma detector, which its output was connected to the pulse counter as shown in Fig. 7. In this experiment, the transmission rate of multiple blocks made of different chemical compounds was measured. For safety reasons, a dosimeter continuously took measurement in the experimental environment. The detector was placed 150 cm from the X-ray source. The material blocks to be measured are placed between the sensor and the X-ray source. The X-ray source was controlled by the relay-interface of the counter presented in this article. The whole experimental setup was monitored from the control room at a safe distance by IP camera. To safely add or remove a new block of material, the X-ray source was stopped by the counter and the operator was able to safely access the experimental setup.

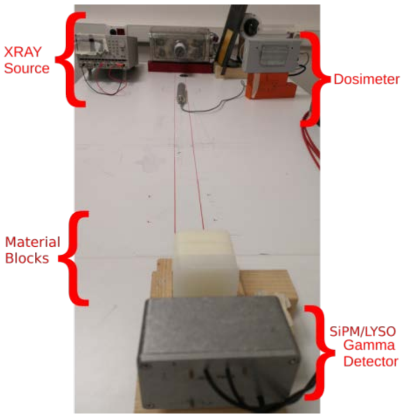

Fig. 7. Experimental setup showing the X-ray source and detector.

Blocks of various materials, each were 10 mm thick, were placed between the source and gamma detector incrementally. When each block was placed in the experimental setup, the pulses received from the sensor were counted by the counter. Transmission rate of photons was detected by the SiPM/LYSO detector and measured by the pulse counter. Actual counts (o marks) and fitting curves theoretically calculated by using Eq.1 (continuous lines) are shown in Fig. 8 for some chemical compounds. Material blocks of 10 mm each were placed in the experimental setup. The transmission rate was measured for 10 seconds for each block. The fluctuation in the count throughout the measurement is shown in the graph with error bars. Material with a total thickness of 20 cm was measured by adding 10 mm blocks to each other. Then, a curve was fitted to the measured values as shown in the figure.

Both catalogues and measured linear attenuation coefficients of selected chemical compounds are given in Table 2. Measured values are calculated by using the fitting curves in Fig. 8 since the thickness is known for the materials. The opposite is also possible. When the linear attenuation coefficient (μ) is known, the thickness of the material can also be found.

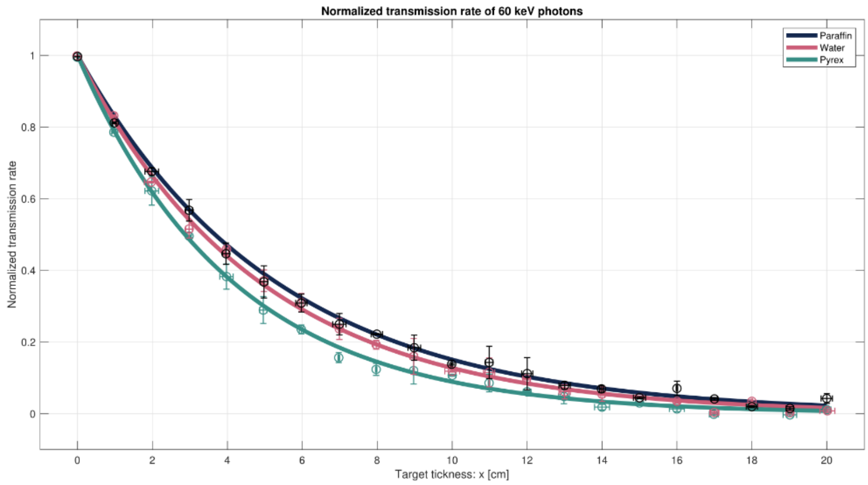

Fig. 8. Normalized transmission rate for chemical compounds.

Table 2. Linear attenuation coefficients of selected chemical compounds.

Linear attenuation coefficient	**Compound**		
	Pyrex	Water	Paraffin
Catalog value [17]	0.2417	0.2059	0.1891
Measured value	0.2397±0.001	0.2053±0.0008	0.1897±0.0007

Results showed that the transmission rates of the given materials could be successfully measured by the pulse counter. Gamma count was inversely proportional to the blocks' thickness and was counted by the pulse counter accurately.

4. Discussion

With the open-source counter design presented in this study, X-ray transmission rate measurement was aimed. Consistent results were obtained in the experiments with the materials given in the Results section. The presented design offers some advantages over its analogues given in the Introduction section. The presented design is a cost effective, easy to implement, handy interface and portable device. It can save data with timestamps, transfer data over the network via TCP, and control external hardware in the experimental setup. However, there are some shortcomings of being low cost. For example, the frequency range is lower compared to some of its counterparts mentioned in references. The design is currently limited to 32-bit 2 channels or 16-bit 4 channels. In order to increase the number of channels, design improvement is required.

The linear attenuation coefficients measured by the counter presented are consistent with actual values. Apart from those used in experiments, different materials can also be measured. However, since photons are scattered more in materials with higher density, the experimental setup should be designed accordingly. Therefore, in this study, experiments have been conducted with basic materials suitable to prove the concept.

One of the advantages of the project is that it has been developed directly in the experimental environment and according to the needs. Other advantages of the system are its ability to save data, send data via TCP protocol, connect to external units via relay-interface, use with touchpad, mouse, or remote-desktop connection. Measurement accuracy and frequency range are close to or better than similar systems.

5. Conclusions

One of the most frequently used methods for measuring material thickness in industry and medical field is transmission rate measurement. Since the mass attenuation coefficients of the elements and chemical compounds are known, it is relatively easy to calculate thickness. However, the measurement equipment is usually costly. In this study, a method to measure transmission rate with a low cost open-source counter is shown in the experimental environment. This method has been shown to be successful in experiments with 3 chemical compounds that can be easily found in the laboratory. For other elements and chemical compounds, measurement can be performed by following the same method. In future studies, it is planned to find the attenuation coefficient of an unknown material with the measurement result. Thus, material determination will be possible.

Nomenclatures

I	Photon intensity
I_0	Initial intensity
x	Photon travel distance in material (mm)

Greek Symbols

μ	Linear attenuation coefficient (cm^{-1})

Abbreviations

BNC	Bayonet Neill–Concelman type connector
DSUB	D-subminiature type connector
LYSO	Lutetium-yttrium Oxyorthosilicate
MCU	Microcontroller Unit
OPamp	Operational Amplifier
RPi	Raspberry Pi SBC
RTOS	Real Time Operating System
SBC	Single Board Computer
SiPM	Silicone Photo Multiplier

References

1. Kim, H.J.; Kim, E.J.; Kim, S.; and Jo, S.C. (2009). Development of multifunctional pulse processing device for sensor signal acquisition. *IEEE Transactions on Nuclear Science*, 56(3), 1184-1187.
2. Kumar, S.V.; and Malathi, M. (2011). Low power synchronous counter using improvised conditional capture flip-flop. *International Conference on Sustainable Energy and Intelligent Systems* (*SEISCON 2011*). Chennai, India, 589-592.
3. Shan, C.; Liu, Y.; and Chen, Z. (2012). Design and application of a digital frequency discriminator constructured by two counters. *IET International*

Conference *on Information Science and Control Engineering 2012* (*ICISCE 2012*). Shenzen, China, 1-4.

4. Jurgo, M.; Kiela, K.; and Navickas, R. (2013). Design of low noise 10 GHz divide by 16…511 frequency divider. *Electronics and Electrical Engineering*, 19(6).
5. Du, B.; Dong, S.; Wang, Y.; Guo, S.; Cao, L.; Zhou, W.; Zuo, Y.; and Liu, D. (2013). High-resolution frequency measurement method with a wide-frequency range based on a quantized phase step law. *IEEE Transactions on Ultrasonics, Ferroelectrics and Frequency Control*, 60(11), 2237-2243.
6. Abdullah, N.I.; Bakar, O.C.; Omar, A.; Murat, Z.H.; and Selamat, M.I. (2013). The screening of human psychological stress using Resonant Field Imaging (RFI) frequency counter. *IEEE International RF and Microwave Conference* (*RFM 2013*). Penang, Malaysia, 382-386.
7. Amirpour, M.; Akbari, S.; Hadidi, K.; and Khoei, A. (2014). New all digital frequency divider and phase shifter. *22nd Iranian Conference on Electrical Engineering* (*ICEE 2014*). Tehran, Iran, 205-208.
8. Rubiola, E.; Lenczner, M.; Bourgeois, P.Y.; and Vernotte, F. (2016). The omega counter, a frequency counter based on the linear regression. *IEEE Transactions on Ultrasonics, Ferroelectrics, and Frequency Control*, 63(7), 961-969.
9. Syahbana, M.A.; Santjojo, D.J.H.D.; and Sakti, S.P. (2016). High-resolution multiple channel frequency counter using spartan-3E FPGA. *International Seminar on Sensors, Instrumentation, Measurement and Metrology* (I*SSIMM 2016*). Malang, Indonesia, 111-114.
10. Ritt, S.; Dinapoli, R.; and Hartmann, U. (2010). Application of the DRS chip for fast waveform digitizing. *Nuclear Instruments and Methods in Physics Research, Section A: Accelerators, Spectrometers, Detectors and Associated Equipment*, 623(1), 486-488.
11. Beltran, A.E. (2013). Low-cost acquisition and development board. An open source hardware proposal. *Symposium of Signals, Images and Artificial Vision*, (*STSIVA 2013*). Bogota, Columbia, 1-4.
12. Zahedi, E. (2013). Quick deployment of open-source hardware and software for a dual-channel biosignal recorder. *IEEE International Conference on Smart Instrumentation, Measurement and Applications* (*ICSIMA 2013*), 1-4.
13. Jin, K.C.; and Song, Y.H. (2016). Open source monitoring hardware for sensor interface. I*nternational Conference on Electronics, Information, and Communications* (*ICEIC 2016*), 1-4.
14. Real, G.E.; Florencia Jaure, M.; and Vitali, A.O. (2018). Data acquisition and industrial control system based on Arduino Due using open-source hardware and software. *XIII Technologies Applied to Electronics Teaching Conference* (*TAEE 2018*), 1-7.
15. Zengin, A.T. (2019). Low-cost open-source high-frequency portable pulse counter for Raspberry Pi and its application to Xray transmission rate measurement. *Journal of Instrumentation*, 14(11), T11004-T11004.
16. Millar, R.H.; and Greening, J.R. (1974). Experimental X-ray mass attenuation coefficients for materials of low atomic number in the energy range 4 to 25 keV. *Journal of Physics B: Atomic and Molecular Physics*, 7(17), 2332-2344.
17. Hubbell, J.H.; and Seltzer, S.M. (1995). Tables of X-ray Mass Attenuation. *National Institute of Standards and Technology* (*NIST*).

18. Kerur, B.R.; Thontadarya, S.R.; and Hanumaiah, B. (1991). A novel method for the determination of X-ray mass attenuation coefficients. *International Journal of Radiation Applications and Instrumentation*, 42(6), 571-575.
19. Withjack, E.M. (1987). Computed tomography for rock-property determination and fluid-flow visualization. *Society of Petroleum Engineers of AIME* (*SPE*), Pi(December), 183-196.
20. Chantler, C.T.; Tran, C.Q.; Barnea, Z.; Paterson, D.; Cookson, D.J.; and Balaic, D.X. (2001). Measurement of the X-ray mass attenuation coefficient of copper using 8.85-20 keV synchrotron radiation. *Physical Review A - Atomic, Molecular, and Optical Physics*, 64(6), 15.
21. Tran, C.Q.; Chantler, C.T.; Barnea, Z.; Paterson, D.; and Cookson, D.J. (2003). Measurement of the X-ray mass attenuation coefficient and the imaginary part of the form factor of silicon using synchrotron radiation. *Physical Review A - Atomic, Molecular, and Optical Physics*, 67(4), 12.
22. Tran, C.Q.; Chantler, C.T.; and Barnea, Z. (2003). X-ray mass attenuation coefficient of silicon: Theory versus experiment. *Physical Review Letters*, 90(25), 257401.
23. De Jonge, M.D.; Barnea, Z.; Tran, C.Q.; and Chantler, C.T. (2004). X-ray bandwidth: Determination by on-edge absorption and effect on various absorption experiments. *Physical Review A - Atomic, Molecular, and Optical Physics*, 69(2), 12.
24. De Jonge, M.D.; Tran, C.Q.; Chantler, C.T.; Barnea, Z.; Dhal, B.B.; Cookson, D. J.; Lee, W. K.; and Mashayekhi, A. (2005). Measurement of the X-ray mass attenuation coefficient and determination of the imaginary component of the atomic form factor of molybdenum over the 13.5-41.5-keV energy range. *Physical Review A - Atomic, Molecular, and Optical Physics*, 71(3), 1-16.
25. Tran, C.Q.; Chantler, C.T.; Barnea, Z.; De Jonge, M.D.; Dhal, B.B.; Chung, C.T.Y.; Paterson, D.; and Wang, J. (2005). Measurement of the X-ray mass attenuation coefficient of silver using the X-ray-extended range technique. *Journal of Physics B: Atomic, Molecular and Optical Physics*, 38(1), 89-107.
26. De Jonge, M.D.; Tran, C.Q.; Chantler, C.T.; Barnea, Z.; Dhal, B.B.; Paterson, D.; Kanter, E.P.; Southworth, S.H.; Young, L.; Beno, M.A.; Linton, J.A.; and Jennings, G. (2007). Measurement of the X-ray mass attenuation coefficient and determination of the imaginary component of the atomic form factor of tin over the energy range of 29-60 keV. *Physical Review A - Atomic, Molecular, and Optical Physics*, 75(3), 1-14.
27. Glover, J.L.; Chantler, C.T.; Barnea, Z.; Rae, N.A.; Tran, C.Q.; Creagh, D.C.; Paterson, D.; and Dhal, B.B. (2008). Measurements of the X-ray mass-attenuation coefficient and imaginary component of the form factor of copper. *Physical Review A - Atomic, Molecular, and Optical Physics*, 78(5), 1-13.
28. Rae, N.A.; Chantler, C.T.; Barnea, Z.; De Jonge, M.D.; Tran, C.Q.; and Hester, J.R. (2010). X-ray mass attenuation coefficients and imaginary components of the atomic form factor of zinc over the energy range of 7.2-15.2 keV. *Physical Review A - Atomic, Molecular, and Optical Physics*, 81(2), 1-10.
29. Singh, K.; Singh, H.; Sharma, V.; Nathuram, R.; Khanna, A.; Kumar, R.; Singh Bhatti, S.; and Singh Sahota, H. (2002). Gamma-ray attenuation coefficients in

bismuth borate glasses. *Nuclear Instruments and Methods in Physics Research, Section B: Beam Interactions with Materials and Atoms*, 194(1), 1-6.

30. Ekinci, N.; and Astam, N. (2007). Measurement of mass attenuation coefficients of biological materials by energy dispersive X-ray fluorescence spectrometry. *Radiation Measurements*, 42(3), 428-430.
31. Ferreira, C.C.; Ximenes, R.E.; Garcia, C.A.B.; Vieira, J.W.; and Maia, A.F. (2010). Total mass attenuation coefficient evaluation of ten materials commonly used to simulate human tissue. *Journal of Physics: Conference Series*, 249.
32. Singh, V.P.; Shirmardi, S.P.; Medhat, M.E.; and Badiger, N.M. (2015). Determination of mass attenuation coefficient for some polymers using Monte Carlo simulation. *Vacuum*, 119, 284-288.
33. Kaçal, M.R.; Akman, F.; and Sayyed, M.I. (2019). Evaluation of gamma-ray and neutron attenuation properties of some polymers. *Nuclear Engineering and Technology*, 51(3), 818-824.
34. Al-Buriahi, M.S.; Arslan, H.; and Tonguç, B.T. (2019). Mass attenuation coefficients, water, and tissue equivalence properties of some tissues by Geant4, XCOM and experimental data. *Indian Journal of Pure and Applied Physics*, 57(6), 433-437.
35. Demir, F.; Budak, G.; Sahin, R.; Karabulut, A.; Oltulu, M.; and Un, A. (2011). Determination of radiation attenuation coefficients of heavyweight- and normal-weight concretes containing colemanite and barite for 0.663 MeV γ-rays. *Annals of Nuclear Energy*, 38(6), 1274-1278.
36. Elmahroug, Y.; Tellili, B.; and Souga, C. (2015). Determination of total mass attenuation coefficients, effective atomic numbers, and electron densities for different shielding materials. *Annals of Nuclear Energy*, 75, 268-274.
37. Almatari, M.; Agar, O.; Altunsoy, E.E.; Kilicoglu, O.; Sayyed, M.I.; and Tekin, H.O. (2019). Photon and neutron shielding characteristics of samarium doped lead alumino borate glasses containing barium, lithium and zinc oxides determined at medical diagnostic energies. *Results in Physics*, 12, 2123-2128.
38. Akman, F.; Kaçal, M.R.; Sayyed, M.I.; and Karataş, H.A. (2019). Study of gamma radiation attenuation properties of some selected ternary alloys. *Journal of Alloys and Compounds*, 782, 315-322.
39. Ekinci, N.; Kavaz, E.; Aygün, B.; and Perişanoğlu, U. (2019). Gamma ray shielding capabilities of rhenium-based superalloys. *Radiation Effects and Defects in Solids*, 174(5-6), 435-451.
40. Kara, H.; Karabul, Y.; Kılıç, M.; İçelli, O.; and Güven Özdemir, Z. (2019). Volcanic rock reinforced epoxy composites for gamma ray shielding. *European Journal of Science and Technology*, 552-560.
41. Akman, F.; Geçibesler, I.H.; Demirkol, I.; and Çetin, A. (2019). Determination of effective atomic numbers and electron densities for some synthesized triazoles from the measured total mass attenuation coefficients at different energies. *Canadian Journal of Physics*, 97(1), 86-92.
42. Miura, I.; Suzuki, R.; Kato, H.; Aoki, T.; Koike, A.; Asami, K.; and Hattori, Y. (2018). Development of Mobil-Robot system for inspecting corrosion under insulation. *The Proceedings of the Symposium on Evaluation and Diagnosis*, 2018.17(0), 204.